ELSEVIER

Journal of Nuclear Materials 245 (1997) 138–146

journal of nuclear materials

# Effects of irradiation and implantation on permeation and diffusion of hydrogen isotopes in iron and martensitic stainless steel

F. Wedig, P. Jung *

*Institut für Festkörperforschung, Association EURATOM-KFA, KFA Jülich, D-52425 Jülich, Germany*

Received 10 January 1997; accepted 20 February 1997

**Abstract**

Permeation and diffusion of hydrogen were measured on virgin and preirradiated iron and martensitic stainless steel with thicknesses of 210 and 810 μm at temperatures from 100° to 400°C. A slight dependence of permeability on thickness and pressure was tentatively ascribed to surface effects. Pressure dependence of diffusivity and deviation from Arrhenius behaviour at low temperatures and/or small thicknesses was consistently described by a model of hydrogen trapping at saturable traps. Preirradiation at room temperature to displacement doses up to $1.5 \times 10^{-3}$ dpa had no influence on permeation but reduced the diffusivity in the steel. Diffusion coefficients were also derived from the time dependence of hydrogen release during implantation. The results show significant differences to the results from permeation measurements. Permeation was strongly increased under penetrative light ion irradiation, probably due to ionization and dissociation of the hydrogen gas on the upstream side.

## 1. Introduction

Interaction of hydrogen with steels is an important problem in a variety of technical applications [1]. In devices for nuclear fusion, the presence of hydrogen can cause problems to many materials with hydrogen embrittlement being of concern especially in ferritic/martensitic steels. This class of steels is favourable due to its improved radiation resistance [2] and its potential of reduced activation [3], but on the other hand features lower solubility and higher diffusivity of hydrogen compared to austenitics.

Hydrogen isotopes may enter structural materials in a fusion reactor mainly from four different sources: (1) implantation from the plasma, (2) from coolants, including hydrogen produced by the radiolysis of water, by aqueous corrosion and hydrogen added as corrosion inhibitor, (3) tritium from breeding and (4) from nuclear reactions of neutrons (transmutations).

Under irradiation conditions, loading and retention of hydrogen isotopes in the structural materials may be significantly modified mainly by two effects: (1) enhanced loading due to dissociation and ionization of the hydrogen gas and (2) altered mobility of the hydrogen in the bulk by irradiation itself or by irradiation induced traps.

It was the aim of the present work to investigate these effects by measuring permeation and diffusion of hydrogen in iron and martensitic stainless steel in virgin and in preirradiated material as well as under simultaneous irradiation and by studying the behaviour of implanted hydrogen.

## 2. Experimental details

The present experiments were performed in an apparatus which is sketched in Fig. 1. The light ion beam from the Jülich Compact Cyclotron passes through a circular aperture (diameter 8 mm, area $A = 5.0 \times 10^{-5}$ m$^2$) and a beam shutter (also used for current measurement). Behind a 24 μm Hastelloy-C window there is an upstream gas volume which can be filled up to a gas pressure of 2 bar. Between this gas volume and the measuring volume is the specimen membrane, mounted between two gold gaskets (open diameter 12 mm, area $A_0 = 1.1 \times 10^{-4}$ m$^2$). The

* Corresponding author.


*PII* S0022-3115(97)00014-7

energy of the hydrogen or deuterium beam can be varied to allow penetration (displacement only) or stopping in the specimen (implantation plus displacement). In the penetration case the beam is measured with an insulated copper beam dump, while for implantation the beam current can only be measured intermittently during beam shut down.

The measuring volume ($V \approx 3.1 \times 10^{-3}$ m$^3$) is pumped by a turbomolecular pump and is equipped with a capacitance pressure gauge (Baratron), an ionization gauge and a quadrupole mass-spectrometer. For technical reasons most of the apparatus is made from stainless steel. Therefore the interaction of hydrogen with the walls of the apparatus must to be taken into account [4,5]. This interaction depends on pressure and can be observed for example by measuring the time dependence of evacuation. For most gases, including noble gases, nitrogen, oxygen and also hydrocarbons, the pressure showed over a wide range an exponential decrease with a time constant given by the ratio of the measuring volume and the pumping speed. For molecular flow of an ideal gas the pumping speed is reciprocal to the square root of the molecular mass. On the other hand for hydrogen isotopes no uniform exponential behaviour was observed and also the initial time constant was much larger than expected from molecular mass. This behaviour was ascribed to interaction of hydrogen with the steel surfaces. It has been shown in previous investigations that the influence of the surface can be reduced by purging the apparatus with hydrogen at elevated temperatures [5,6]. The main steps of the treatment used in the present work were baking of the apparatus at $\approx$ 250°C for 24 h, filling with 1 bar hydrogen at 250°C for 1/2 h, evacuating plus baking for 12 h and finally cooling down to room temperature. Fig. 2 shows the decay of the hydrogen signals of the mass spectrometer during a permeation experiment after a sudden reduction of gas pressure in a purged and unpurged apparatus, respectively. A corresponding delay of the signal is observed in the unpurged apparatus when the pressure is raised, for more details cf. Ref. [7]. These wall effects on response time of the measuring device and its

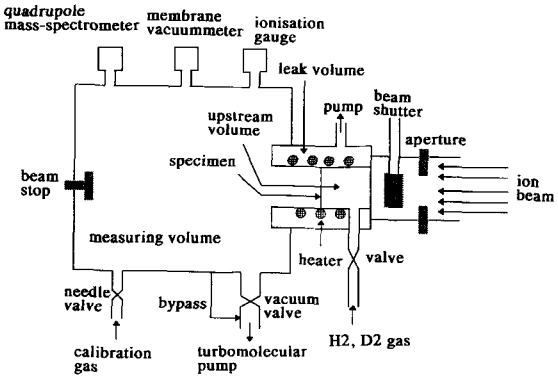


Fig. 1. Schematic view of the permeation apparatus for simultaneous irradiation or implantation.

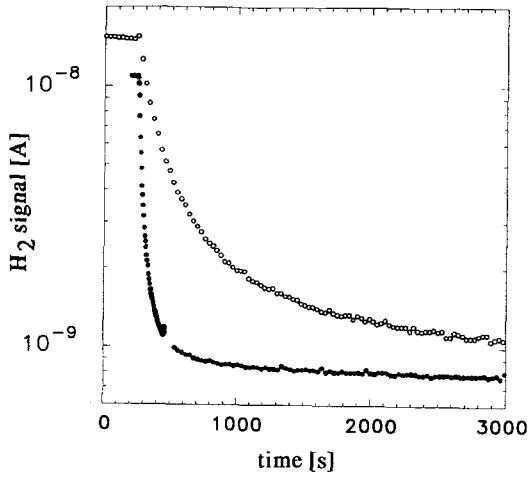


Fig. 2. Time dependence of the $H_2$ measuring signal in Ampères at the end of a permeation measurement at 200°C of a MANET II specimen in an unpurged (○) and a purged (●) apparatus.

possible reduction by previous hydrogen cycles may sham irreversible trapping in the specimen. For previous discussions on this controversial question cf. Refs. [8–10]. Certainly, trapping in the bulk must be taken into account when delayed permeation shows a distinct dependence on alloy composition under otherwise identical experimental conditions [8,11]. But even in this case contributions of wall effects may affect the absolute values. Furthermore dissociation and recombination of the permeating gas at the surfaces may become time limiting at low temperatures [12,13]. More details on this topic will be given in Section 6.

To keep the wall effects and especially their variations during the experiments to a minimum, permeation was studied while the measuring volume was pumped with a pumping speed $S \approx 2 \times 10^{-3}$ m$^3$/s. The permeation flux $\phi$ (mol/m$^2$ s) is then derived from the stationary increment of downstream pressure $\Delta p_2$ (Pa) by

$$\phi = \frac{\Delta p_2 S}{A_0 RT}, \tag{1}$$

with $R = 8.314$ J/K mol and $T$ (K) the temperature of the measuring volume. After a change of upstream pressure $p_1$ a flux transient of $\phi(t)$ occurred with a half-time $\tau_{1/2}$, which for diffusion controlled permeation is related to the effective diffusivity $D^*$ (m$^2$/s), i.e., diffusion including possible trapping, by

$$\tau_{1/2} = \frac{ad^2}{\pi^2 D^*}, \tag{2}$$

with [14]

$$\sum_1^\infty (-1)^n \exp(-an^2) = -\frac{1}{4}, \quad \text{i.e., } a \approx \ln 4.$$

$d$ (m) is the specimen thickness. For a numerical solution of this diffusion problem refer to Ref. [15]. The mass-spectrometer was calibrated from $< 10^{-4}$ to $5 \times 10^{-3}$ Pa against the ionisation gauge, which in turn was calibrated against the capacitance gauge from $10^{-3}$ to 1 Pa. Linear dependence of the mass-spectrometer signal on pressure is limited to values below $5 \times 10^{-3}$ Pa.

Materials in the present investigation were 99.99% pure iron from Goodfellow and the reference martensitic steel (MANET II) from the European fusion programme. The main constituents (wt%) of MANET II are 86.3 Fe, 10.3 Cr, 0.78 Mn, 0.67 Ni, 0.57 Mo, 0.2 V, 0.19 Si, 0.12 Nb, 0.10 C and 0.024 N. Iron specimens of 210 μm thickness were annealed for 1 h at 750°C, while the MANET II steel received the standard heat treatment (1/2 h at 1075°C/quench/2 h at 750°C/furnace cooling) after rolling in steps of ≤ 25% cold reduction to thicknesses of 210 and 810 μm.

Some specimens were preirradiated with protons in the 10 MeV range. The specimens were soldered with a low temperature solder to a copper heat sink, i.e., specimen temperature during irradiation and unsoldering was ≤ 80°C. After half the dose the specimens were turned around to improve damage homogeneity. Displacement doses and ranges of implanted ions were derived from Monte Carlo calculations [16].

## 3. Permeation

Under the assumption of diffusion controlled flux $\phi$, apparent permeabilities $P^*$ are given by Richardson's law:

$$P^* = \frac{\phi d}{\sqrt{p_1}}. \tag{3}$$

Permeability data of MANET II as a function of pressure are compiled in Fig. 3. At least above $10^3$ Pa, the values in Fig. 3 are independent of pressure in agreement with Eq. (3), while dominance of surface reactions would give a $\sqrt{p}$ dependence as indicated by the dashed line [12]. On the other hand the apparent permeabilities of the 810 μm MANET specimens are clearly higher by a factor of ≈ 1.35 compared to 210 μm. Corresponding results are obtained for iron [7]. Apparent permeabilities as a function of temperature are given in Fig. 4. There is no significant effect of preirradiation, neither in MANET nor Fe, at least up to the present maximum dose of $1.5 \times 10^{-3}$ dpa. The apparent permeabilities in mol/m s $\sqrt{\text{Pa}}$ can be described by

For 210 μm MANET II:

$$P^*_{H_2} = 3.1 \times 10^{-8} \exp(-41\,500/\text{RT})$$
$$427 \le \text{T (K)} \le 730, \tag{4a}$$

$$P^*_{D_2} = 3.2 \times 10^{-8} \exp(-41\,600/\text{RT})$$
$$427 \le \text{T (K)} \le 730; \tag{4b}$$

for 810 μm MANET II:

$$P^*_{H_2} = 4.1 \times 10^{-8} \exp(-40\,800/\text{RT})$$
$$427 \le \text{T (K)} \le 730, \tag{4c}$$

$$P^*_{D_2} = 7.0 \times 10^{-8} \exp(-43\,400/\text{RT})$$
$$427 \le \text{T (K)} \le 730; \tag{4d}$$

and for 210 μm iron:

$$P^*_{H_2} = 3.1 \times 10^{-8} \exp(-34\,500/\text{RT})$$
$$378 \le \text{T (K)} \le 578, \tag{5a}$$

$$P^*_{D_2} = 3.6 \times 10^{-8} \exp(-43\,100/\text{RT})$$
$$360 \le \text{T (K)} \le 388. \tag{5b}$$

When during a permeation experiment the specimens were simultaneously irradiated with penetrating protons, the eventual stationary hydrogen signal in the measuring volume showed a linear increase with beam current. The ratio of additional permeation current $\Delta\phi_p$ to proton beam current $\phi_i$ is shown in an Arrhenius plot in Fig. 5 for MANET II and iron. For plotting this ratio it was assumed that the permeation through the unirradiated area $(A_0 - A)$ is not altered by irradiation of area $A$. The ratios are by about an order of magnitude larger for iron than for

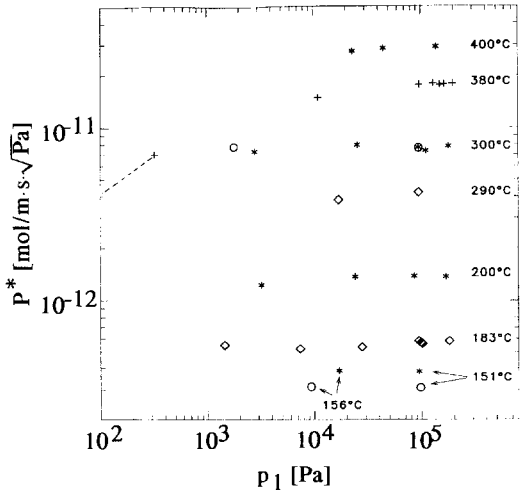


Fig. 3. Apparent permeabilities (Eq. (3)) of $H_2$ and $D_2$ in MANET II specimens of thicknesses of 210 μm ($H_2$: +, $D_2$: ◇) and 810 μm ($H_2$: *, $D_2$: ○) as a function of upstream pressure $p_1$. The data at 400°C are from a specimen preirradiated to $9 \times 10^{-5}$ dpa.

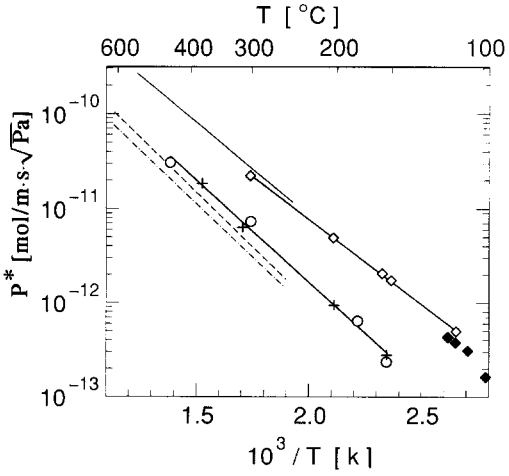


Fig. 4. Temperature dependence of apparent permeabilities of $H_2$ (◇) and $D_2$ (◆) in 210 μm iron irradiated up to $1.5\times10^{-3}$ dpa and of $H_2$ in 210 μm MANET II unirradiated (+) and irradiated with 12.3 MeV protons to $1.5\times10^{-3}$ dpa (○), respectively. Included are averaged literature data for $H_2$ in iron (-) [21] and in DIN1.4914 (–) and MANET I (-·-) [22].

MANET II. For a typical beam current of 500 nA (≈ 10 nA/mm$^2$) the permeabilities can be described by

For 210 μm MANET II:

$$P^*_{H_2,D_2} = 1.5\times10^{-8}\exp(-35\,700/RT)$$
$$455 \le T\,(K) \le 645 \qquad (6)$$

and for 210 μm iron:

$$P^*_{D_2} = 2.1\times10^{-8}\exp(-36\,700/RT)$$
$$357 \le T\,(K) \le 427. \qquad (7)$$

Comparison of Eqs. (6) and (7) to Eqs. (4a), (4b), (4c), (4d) and (5b) shows that the prefactors and the activation energies are reduced under the 500 nA irradiation by about 50% and ≈ 14%, respectively.

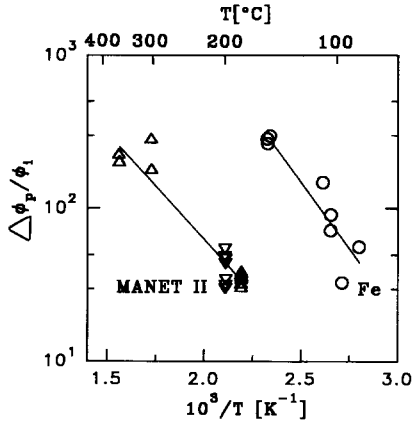


Fig. 5. Ratio of additional permeation current $\Delta\phi_p$ to proton beam current $\phi_i$ as a function of temperature for an upstream pressure of $10^5$ Pa through 210 μm iron (○) and through 210 μm (△) and 810 μm MANET II (▽).

## 4. Diffusion

Apparent diffusivities of $H_2$ and $D_2$ in virgin and preirradiated MANET II derived from transients during pressure changes using Eq. (2) are shown in Fig. 6 as a function of pressure for different temperatures and specimen thicknesses. Values derived from pressure increase and decrease were equal within experimental error, cf. Ref. [17]. The effect of isotope mass was slightly smaller than the expected factor of $\sqrt{2}$, as also observed in previous investigations [18]. Effect of pressure and preirradiation on diffusion is much larger than for permeation, cf. Figs. 3 and 4. For the 210 μm iron specimens the time constants $\tau_{1/2}$ even at temperatures around 100°C were in the order of only a few seconds and therefore diffusivities could not be precisely determined in the present apparatus. Determination of diffusivities under simultaneous irradiation was not possible due to lack of beam stability.

## 5. Implantation

In the implantation experiments the upstream volume was evacuated and the specimens were irradiated with

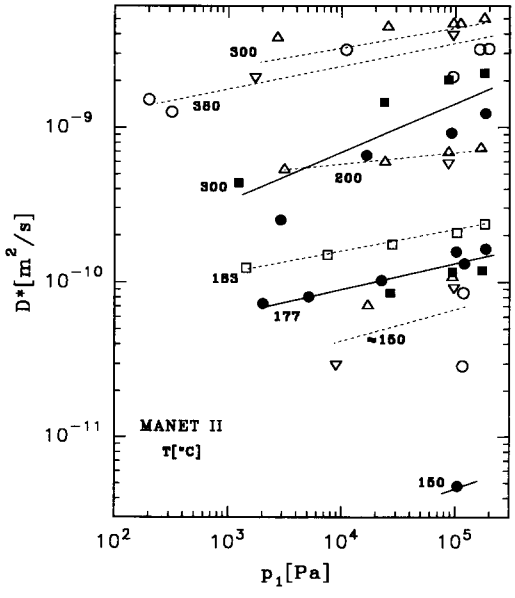


Fig. 6. Apparent diffusivities in unirradiated (open symbols, dashed lines) and preirradiated ($1.5\times10^{-3}$ dpa, filled symbols, solid lines) MANET II as function of upstream pressure $p_1$. Circles and squares indicate diffusion of $H_2$ (○, ●) and $D_2$ (□, ■) in 210 μm specimens and triangles $H_2$ (△) and $D_2$ (▽) in 810 μm specimens, respectively.

protons of ranges $r$ smaller than specimen thickness $d$. The hydrogen flux $\phi_p$ permeating to the measuring volume was proportional to the implantation current $\phi_i$. According to Fick's first law the fraction $f_r = \phi_p/\phi_i$ of implanted ions diffusing to the measuring volume is given by $r/d$ (dashed line in Fig. 7). Most of the measured fractions in Fig. 7 (averaged over several measurements) are below this relation and furthermore a slight decrease of the released fraction could be detected during implantation.

From the time evolution of the mass spectrometer signal at the beginning and the end of implantation, diffusion coefficients were derived, cf. Ref. [19]. For implantation close to the downstream surface the following relation is approximately obtained from solution of the diffusion equation:

$$D^* = \frac{(d-r)^2}{b\epsilon\tau_{1/2}}, \tag{8}$$

with $\mathrm{erfc}(\sqrt{b}/2) = 0.5$, i.e., $b \approx 0.97$ [20]. $1/\epsilon$ approximates the total released fraction of the implanted atoms, i.e., $1/\epsilon \approx f_r d/r$, while a fraction $\approx (1 - 1/\epsilon)$ is retained by trapping or clustering. For implantation further away from the surface, Eq. (8) must be replaced by numerical calculations which for example give for implantation into the centre of the specimen ($r \approx d/2$) [19]:

$$D^* = \frac{(d/2)^2}{2.6\epsilon\tau_{1/2}}. \tag{9}$$

The diffusion coefficients show significant scatter, probably mostly due to beam fluctuations, but indicate no systematic dependence on implantation current. $D^*$ values derived at the beginning and at the end of an implantation period are given in Fig. 8. Values at the end are systematically higher, especially for implantations close to the backside surface and for low temperatures.

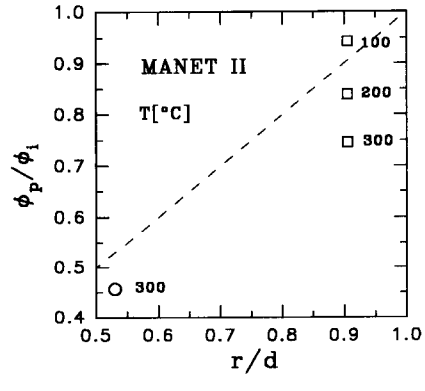


Fig. 7. Ratio of hydrogen flux permeating to the downstream side $\phi_p$ to the proton flux $\phi_i$ implanted in 810 μm MANET II, as a function of relative implantation depth at temperatures as indicated. Proton energies were 15 MeV for $r/d = 0.53$ and 20 MeV for $r/d = 0.91$, respectively. The dashed line gives the prediction by Fick's first law.

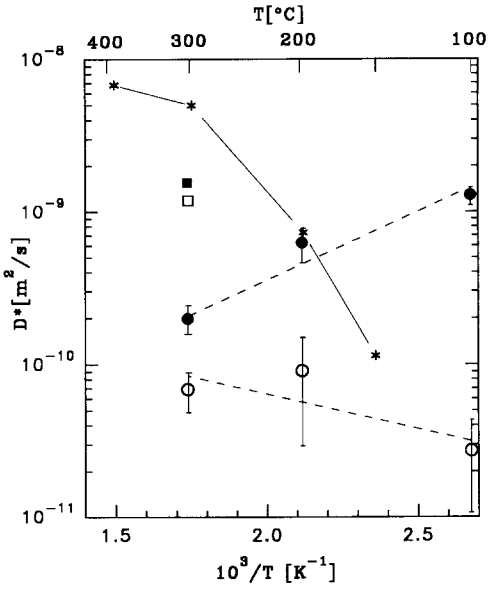


Fig. 8. Diffusion coefficients as a function of temperature derived from release of hydrogen implanted in 810 μm MANET II to relative depths $r/d$ of 0.53 (□, ■) and 0.91 (○, ●). Data are taken at the beginning (open symbols) and end (filled symbols) of implantation. The errors bars give standard deviations. Included are diffusion coefficients derived from permeation experiments (*, see Fig. 10).

## 6. Discussion

The present results on the *permeability* of iron and MANET I are in reasonable agreement with literature data, Refs. [21,22], which are included in Fig. 4. The slightly higher permeability of MANET II compared to the two heats investigated in Ref. [22] may be due to the lower Cr content of the present material, refer to Ref. [23].

Some of the present apparent permeabilities derived from Eq. (3) show dependence on pressure and on thickness, cf. Eqs. (4a), (4b), (4c) and (4d), i.e., deviations from Richardson's law. This may be due to one or both of the following reasons:

(1) Dissociation and recombination processes at the surfaces become rate limiting in comparison to bulk diffusion.

(2) Diffusion in surface barriers (oxides etc.) with much lower diffusivity than the bulk metal becomes rate limiting.

In the latter case, due to the higher diffusion energy of barriers, cf. Ref. [24], the ratio of permeabilities through specimens with different thickness should increase with decreasing temperature, in contrast to the present results. Furthermore dominance of diffusion through barriers can-

not explain the observed pressure dependence of apparent permeabilities. Also in other ferritic/martensitic [25–28] and in austenitic [29,30,25] materials deviations from Richardson's law, mainly at low temperatures and pressures, have been explained by dissociation and recombination processes at the surfaces becoming rate controlling. But the present deviations from Richardson's law and the span of investigated thicknesses and pressures, compared to error margins, are too small to allow a quantitative comparison to theoretical models, cf. [12,31,32]. In any case the small differences indicate that the present high thickness/high pressure data are at maximum a few 10% below the bulk values.

*Permeation under irradiation* (Fig. 5) increases linearly with beam current and shows less temperature dependence than without irradiation. The additional permeation induced per irradiation particle is seemingly independent of thickness and around 200°C it is about one order of magnitude higher in Fe than in MANET. A maximum in irradiation induced permeation, which in the literature is commonly referred to as 'permeation spike' [33], could not be detected within the variations of beam current.

Mainly three techniques were applied so far to simulate the flux of atomic hydrogen in a fusion environment in so-called ion- or plasma-driven permeation experiments (IDP or PDP), cf. Refs. [12,34–37].

(1) Atomic hydrogen was produced by a heated filament in front of the permeation membrane [27] or by gas discharge [38]. In this case the atomic hydrogen has essentially thermal energies and no damage is introduced to the specimen. Slightly higher energies up to $\approx 500$ eV are obtained by radiofrequency and combined radiofrequency plus glow discharge [39,40].

(2) Shallow implantation of ionized hydrogen isotopes in the keV energy range, cf. Refs. [37–42]. In this case the atomic hydrogen isotopes are energetically implanted into the specimen, causing damage up to a depth corresponding to the range of the ions.

(3) In situ irradiation by $\gamma$ radiation [43,44], $\alpha$ particles [45] or neutrons [46–51]. While the hydrogen molecules have virtually thermal energy, they may be dissociated and/or ionized and furthermore the irradiation may produce radiation damage in the specimen. The latter type of experiments is most closely related to the present case. While hydrogen permeation in type 316 stainless steel was not changed by a $3.7 \times 10^7$ Bq $^{60}$Co $\gamma$-source close to the upstream surface under 0.1 bar $H_2$ [43], a $^{233}$U $\alpha$-source of $3 \times 10^{10}$ Bq at a distance of 0.1 m under 1 bar $H_2$ increased the permeation rate and reduced its activation energy in pure (99.94%) iron [45]. Also the in-pile experiments on various austenitic stainless steels gave enhanced permeation and reduced activation energies [46–51].

Models of permeation under irradiation have been elaborated mainly by groups at KFA [12,32] and Sandia [34,52], mostly addressing experiments of the first two types above. The present experimental situation differs too much from those models to allow a detailed comparison. The following mechanisms are discussed to explain the enhanced permeation under ionizing irradiation:

(1) Enhanced uptake of dissociated and/or ionized hydrogen at the front surface, or alternatively dissociation of adsorbed hydrogen molecules [40],

(2) Enhanced diffusion in the bulk [33].

With respect to the first possibility, the ionization capabilities of various particles can be estimated from the product of stopping power $dE/dx$ and particle flow rate $\Gamma$ (Table 1). From the products $\Gamma\, dE/dx$ in Table 1 it can be understood why practically no enhancement of permeation was observed under $\gamma$ irradiation and why the $\alpha$ irradiation in Ref. [45] and the present proton irradiations give similar enhancements. The slightly higher enhancement in Fe compared to MANET cannot be explained by this consideration. The ratios of permeation rates with and without proton irradiation $P_{irr}/P$ decrease slightly with increasing temperature. In other words the apparent activation energy is reduced under irradiation (compare Eqs. (6) and (7) to Eqs. (4a), (4b), (4c), (4d) and (5b)). Such behaviour was also observed in the case of hydrogen permeation through iron under simultaneous $\alpha$ irradiation [45]. Reactor irradiations on austenitic stainless steels show that the enhancement of diffusion under irradiation is stronger than the effect on permeation [49,51].

The present method for measuring *diffusion*, cf. Eq. (2), is a modified version of the widely used time lag

Table 1
Ionization capabilities ($\Gamma\, dE/dx$) of various sources in $10^5$ Pa $H_2$ gas (mass density $\theta = 8.9 \times 10^{-2}$ kg/m$^3$), derived from particle rate $\Gamma$ and energy loss $dE/dx$, compared to experimental ratios of permeabilities with and without irradiation ($P_{irr}/P$)

| Target | $T$ (°C) | Particle | Source | $E$ (MeV) | $\Gamma$ (1/s) | $dE/dx$ (eV/m) | $\Gamma\, dE/dx$ | $P_{irr}/P$ | Ref. |
|---|---|---|---|---|---|---|---|---|---|
| SS316 | > 150 | $\gamma$ | $^{60}$Co | 1.3 | $3.7 \times 10^7$ | $\approx 7 \times 10^{2}$ [a] | $3 \times 10^{10}$ | 1.01 | [43] |
| Fe | 450 | $\alpha$ | $^{233}$U | $\approx 5$ | $3 \times 10^{10}$ | $\approx 1 \times 10^{7}$ [b] | $3 \times 10^{17}$ | 1.5 | [45] |
| Fe | 80 | p-500nA | cyclotron | 10 | $3.1 \times 10^{12}$ | $\approx 5 \times 10^{5}$ [c] | $1.4 \times 10^{17}$ | 5 | [7] |
| MANET | 180 | p-500nA | cyclotron | 10 | $3.1 \times 10^{12}$ | $\approx 5 \times 10^{5}$ [c] | $1.4 \times 10^{17}$ | 2 | [7] |

[a] $dE/dx \approx E\mu$, with mass attenuation coefficient $\mu/\theta \approx 6 \times 10^{-3}$ m$^2$/kg.
[b] Ref. [76].
[c] Ref. [77].

method [53–55]. The above mentioned effects of surface reactions on permeation also affect diffusion measurements. But the strong deviation from Arrhenius behaviour and the much stronger dependence of diffusivity on thickness and pressure compared to steady state permeation indicate that also other processes become important. The increase of diffusivity with increasing thickness qualitatively coincides with previous results on iron, cf. Refs. [56,57], as does the pressure dependence [58,59]. Also the strong deviation from Arrhenius law of diffusivity is in accord with similar results for iron [60,61] and steels [62–64]. But the present investigation on MANET seems to be the first one to measure both, pressure and temperature dependence, of diffusivity on one material.

Models of reversible trapping at microvoids [57,65] are at variance with the present results, while a consistent explanation of the dependence on pressure and temperature is possible with a model for capturing of hydrogen atoms at saturable traps, cf. Refs. [53,58]. The treatment in Ref. [53] gives the ratio of lattice diffusivity $D$ (i.e., without trapping) to the effective diffusion coefficient $D^*$:

$$\frac{D}{D^*} = 1 + \frac{3\alpha}{\beta}\left(1 + \frac{2}{\beta}\left(1 - \left(1 + \frac{1}{\beta}\right)\ln(1+\beta)\right)\right). \tag{10}$$

$\alpha = (n_T/n_L)\exp(E_b/RT)$, with $n_T$ the trap density, $n_L$ the density of sites for hydrogen diffusion ($n_L = 6n_0 \approx 5 \times 10^{29}$ m$^{-3}$ for tetrahedron sites, with $n_0$ the number density of lattice atoms) and $E_b$ the average binding energy to a trapping site. $\beta = (n_H/n_L)\exp(E_b/RT)$ gives the trap occupancy, with $n_H$ as the density of hydrogen atoms. With Sieverts' law ($n_H = Sp^{1/2}$), Eq. (10) can be used to plot $D/D^* - 1$ versus $p^{-1/2}$ (Fig. 9). For high pressures ($\beta \gg 1$) one obtains $D/D^* - 1 \approx 3\alpha/\beta = 3n_T/n_H$, i.e., a straight line with slope $3n_T/S$, while for low pressures ($\beta \ll 1$) a constant value $D/D^* - 1 \approx \alpha$ (using $\ln(1+\beta) \approx \beta - \beta^2/2 + \beta^3/3$) is approached. In the temperature range 177–200°C, for unirradiated MANET an atomic trap concentration $n_T/n_0 \approx 4 \times 10^{-6}$ is obtained, while irradiated specimens ($1.5 \times 10^{-3}$ dpa) give by about a factor of two higher values. The binding energies are uniformly $\approx 65$ kJ/mol. A comparison to binding energies of hydrogen to various traps in iron and ferritic/martensitic steels indicates that probably in both cases vacancies are the major traps [66–68]. At temperatures above 300°C the initial slopes and asymptotic values cannot be safely determined (Fig. 9). Rough estimates give lower $n_T/n_0$ values by about a factor of 1.4 than those at 177–200°C and $E_b = 82$ kJ/mol.

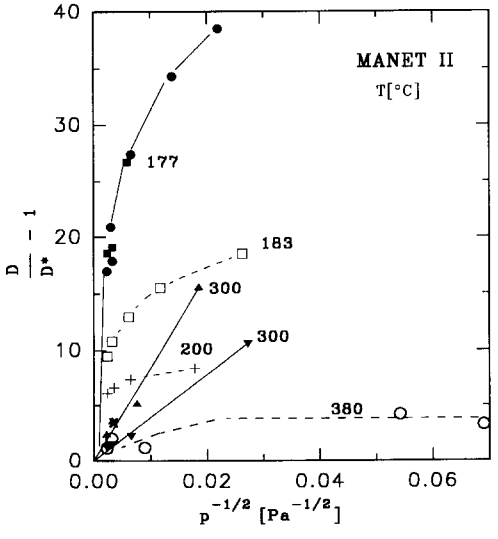


Fig. 9. Evaluation of lattice diffusion coefficients $D$ from the pressure dependence of apparent diffusivities $D^*$ of MANET II (cf. Fig. 3). Specimen thicknesses were 210 μm (H: ○, D: □) and 810 μm (H: +, D: ×). Solid symbols indicate 210 μm specimens preirradiated to $1.5 \times 10^{-3}$ dpa (H: ●, ▼; D: ■, ▲).

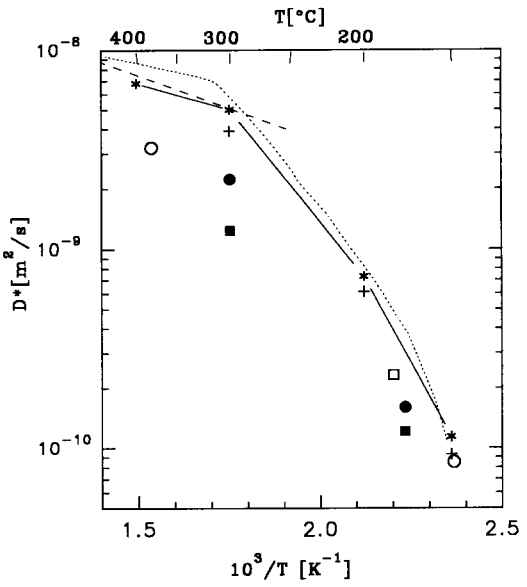


Fig. 10. Temperature dependence of diffusion coefficients of hydrogen isotopes in MANET II, derived from permeation experiments. Symbols indicate diffusion of $H_2$ and $D_2$ in 210 μm (○, □) and 810 μm (*, +) specimens, respectively. Filled symbols (●, ■) indicate diffusion in 210 μm specimens preirradiated to $1.5 \times 10^{-3}$ dpa. Included are literature data for MANET I (–) [22] and for Japanese JFMS steel (· · ·) [75].

A compilation of diffusion coefficients derived from the present permeation experiments is given in Fig. 10. As in previous investigations on MANET II [69], iron [70], steels [62,65,67,71,72] and in low activation F82H [73] the present diffusion coefficients approach an Arrhenius behaviour, i.e., $D = D_0\exp(-E_m/RT)$, only above $\approx$

300°C, with $D_0 \approx 4.5 \times 10^{-8}$ m$^2$/s and $E_m \approx 10$ kJ/mol H. At lower temperatures diffusivities deviate from this relation and can be described according to the saturable trap model, cf. Eq. (10), by

$$D^* \approx \frac{D}{1+\alpha}. \tag{11}$$

For an alternative description refer to Ref. [74]. The data of the unirradiated 810 μm specimens in Fig. 10 can be fitted with an atomic trap concentration $n_T/n_0 \approx 2 \times 10^{-6}$ of traps and an average binding energy $E_b \approx 63$ kJ/mol. These values are in reasonable agreement with the above values derived from the pressure dependence.

The reduced release of hydrogen during *implantation* (Fig. 7) is probably due to retention by trapping at irradiation defects, i.e., $1/\epsilon < 1$ in Eqs. (8) and (9). A further decrease of $1/\epsilon$ during the course of implantation, which could not be measured precisely and therefore was not included in the calculations of $D^*$ by Eqs. (8) and (9), may at least partially account for the increase of the $D^*$s at the end of implantation (Fig. 8). An alternative explanation would be surface effects becoming more important. In this case the higher concentration of retained hydrogen towards the end of implantation would cause higher surface reaction rates (quadratic dependence on $n_H$) and therefore higher apparent diffusion coefficients [7].

## 7. Conclusions

(1) Hydrogen diffusivity in iron and martensitic MANET II shows a pronounced dependence on gas pressure and a deviation from Arrhenius type temperature dependence at temperatures below 300°C.

(2) These pressure dependences can be quantitatively described by a model of saturably trapping at vacancies with a binding energy of about 65 kJ/mol and an atomic trap concentration of about 4 atppm.

(3) Almost identical binding energies and trap concentrations were derived from the temperature dependence of the diffusion coefficients.

(4) Preirradiation to a displacement dose of $1.5 \times 10^{-3}$ dpa has only a negligible effect on permeation of hydrogen in iron and MANET II.

(5) The preirradiation affects diffusivity by increasing the trap concentration by about a factor of 2, while the binding energy remains virtually unchanged.

(6) Simultaneous irradiation with light ions enhances hydrogen permeability, probably due to dissociation/ionisation of the gas.

(7) Diffusion coefficients derived from measurements of the release of implanted hydrogen differ from the results from the permeation experiments and show not fully understood differences between beginning and end of implantation.

## References


[1] J.P. Hirth, Metall. Trans. 11A (1980) 861.
[2] J.W. Davis, D.J. Michel, eds., Topical Conf. on Ferritic Alloys for use in Nuclear Energy Technol., Snowbird 1983, Met. Soc. AIME, 1984.
[3] K. Ehrlich, S. Kelzenberg, H.-D. Röhrig, L. Schäfer, M. Schirra, J. Nucl. Mater. 212–215 (1994) 678.
[4] H.P. Buchkremer, PhD thesis RWTH Aachen, Report KFA Jülich Jül-1806 (1982).
[5] E. Rota, PhD thesis, University of Düsseldorf, Report KFA Jülich Jül-2041 (1986).
[6] E. Rota, thesis tesa di laurea, University of Turin (1979–1980).
[7] F. Wedig, thesis RWTH Aachen, Report KFA Jülich Jül-3334 (1997).
[8] I.M. Bernstein, A.W. Thompson, in: Advanced Techniques for Characterizing Hydrogen in Metals, eds. N.F. Fiore and B.J. Berkowitz (Metallurgical Society of AIME, 1982) p. 89.
[9] R.-W. Lin, H.H. Johnson, in: Advanced Techniques for Characterizing Hydrogen in Metals, eds. N.F. Fiore and B.J. Berkowitz (Metallurgical Society of AIME, 1982) p. 105.
[10] M.R. Shanaberger, A. Taslami, H.G. Nelson, Scr. Metall. 15 (1981) 929.
[11] S.L.I. Chan, H.L. Lee, J.R. Yang, in: Hydrogen Effects on Material Behaviour, eds. N.R. Moody and A.W. Thompson (The Minerals, Metals and Materials Society, 1990) p. 145.
[12] F. Waelbroeck, P. Wienhold, J. Winter, E. Rota, T. Banno, Report KFA Jülich Jül-1966 (1984).
[13] D.K. Kuhn, M.R. Shanaberger, in: Hydrogen Effects on Material Behaviour, eds. N.R. Moody and A.W. Thompson (The Minerals, Metals and Materials Society, 1990) p. 33.
[14] J. Crank, The Mathematics of Diffusion (Oxford, 1966).
[15] P. Wienhold, M. Profant, F. Waelbroeck, J. Winter, Report KFA Jülich, Jül-1825 (1983).
[16] J.P. Biersack, L.G. Haggmark, Nucl. Instrum. Methods 174 (1980) 257.
[17] R.C. Frank, D.E. Swets, D.L. Fry, J. Appl. Phys. 29 (1958) 892.
[18] R.C. Frank, R.W. Lee, R.L. Williams, J. Appl. Phys. 29 (1958) 898.
[19] P. Jung, Nucl. Instrum. Methods B91 (1994) 362.
[20] V. Philipps, Report KFA Jülich Jül-1679 (1980).
[21] O.D. Gonzales, Trans. Metall. Soc. AIME 245 (1969) 607.
[22] K.S. Forcey, D.K. Ross, J.C.B. Simpson, D.S. Evans, J. Nucl. Mater. 160 (1988) 117.
[23] P. Jung, J. Nucl. Mater. 238 (1996) 189.
[24] P. Jung, in: Diffusion Processes in Nuclear Materials, ed. R.P. Agarwala (Elsevier, Amsterdam, 1992) p. 235.
[25] H.D. Röhrig, R. Hecker, J. Blumensaat, J. Schaefer, J. Nucl. Mater. 34 (1975) 157.
[26] P.L. Chang, W.D.G. Bennett, J. Iron Steel Inst. 170 (1952) 205.
[27] F. Waelbroeck, I. Ali-Khan, K.J. Dietz, P. Wienhold, J. Nucl. Mater. 85&86 (1979) 345.
[28] E. Serra, A. Perujo, J. Nucl. Mater. 223 (1995) 157.
[29] E. Rota, F. Waelbroeck, P. Wienhold, J. Winter, J. Nucl. Mater. 111&112 (1982) 233.
[30] D.M. Grant, D.L. Cummings, D.A. Blackburn, J. Nucl. Mater. 152 (1988) 139.
[31] R. Ash, R.M. Barrer, Philos. Mag. 47 (1959) 1197.

[32] P. Wienhold, E. Rota, F. Waelbroeck, J. Winter, T. Banno, Report KFA Jülich Jül-2079 (1986).
[33] T. Tanabe, Defect Diffus. Forum 95–98 (1993) 317.
[34] D.K. Brice, B.L. Doyle, J. Vac. Sci. Technol. A5 (1987) 2311.
[35] R.A. Kerst, W.A. Swansinger, J. Nucl. Mater. 122&123 (1984) 1499.
[36] K.L. Wilson, B. Bastasz, R.A. Causey, D.K. Brice, B.L. Doyle, W.R. Wampler, W. Möller, B.M.U. Scherzer, T. Tanabe, Nucl. Fusion (Suppl.) 1 (1991) 31.
[37] T. Nagasaki, M. Saidoh, R. Yamada, H. Ohno, J. Nucl. Mater. 202 (1993) 228.
[38] A.I. Lifshitz, M.E. Notkin, Y.M. Pustovoit, A.A. Samartsev, Vacuum 29 (1979) 113.
[39] T. Tanabe, N. Saitoh, Y. Etoh, S. Imoto, J. Nucl. Mater. 103&104 (1981) 483.
[40] R.A. Causey, D.F. Holland, M.L. Sattler, Nucl. Tech./Fusion 4 (1983) 64.
[41] V.M. Sharapov, A.V. Zakharov, V.V. Matveev, Sov. Phys. Tech. Phys. 20 (1976) 1262.
[42] T. Tanabe, Y. Yamanishi, S. Imoto, Trans. Jpn. Inst. Met. 25 (1984) 1.
[43] E.H. van Deventer, V.A. Maroni, J. Nucl. Mater. 92 (1980) 103.
[44] R.A. Causey, L.M. Steck, J. Nucl. Mater. 122&123 (1984) 1518.
[45] R.R. Heinrich, C.E. Johnson, C.E. Crouthamel, J. Electrochem. Soc. 112 (1965) 1067.
[46] G.W. Schwarzinger, R. Dobrozemsky, J. Nucl. Mater. 122& 123 (1984) 1560.
[47] G. Schwarzinger, R. Dobrozemsky, in: Proc. Symp. on Atomic and Surf. Physics, 1982, eds. W. Lindinger et al., p. 129
[48] R. Dobrozemsky, G. Schwarzinger, C. Stratowa, in: Proc. 8th Int. Vacuum Congr., 1980, Cannes, vol. II, eds. J.P. Langeron and L. Maurice (Societé Française de Vide) p. 15.
[49] B.G. Polosukhin, E.P. Baskakov, E.M. Sulimov, A.P. Zyrianov, Y.S. Shestakov, G.M. Kalinin, Y.S. Strebkov, A.G. Dobrynskih, J. Nucl. Mater. 191–194 (1992) 219.
[50] B.G. Polosukhin, E.M. Sulimov, A.P. Zyrianov, G.M. Kalinin, Fusion Technol. 28 (1995) 1268.
[51] I.L. Tazhibaeva, V.P. Shestakov, E.V. Chikhray, O.G. Romanenko, A.K. Klepikov, Y.S. Cherepnin, E.A. Kenzhin, A.A. Basov, A.A. Kolodeshnikov, Fusion Technol. 28 (1995) 1290.
[52] D.K. Brice, B.L. Doyle, J. Nucl. Mater. 120 (1984) 230.
[53] A. McNabb, P.K. Foster, Trans. Met. Soc. AIME 227 (1963) 619.
[54] H.J. Frisch, J. Phys. Chem. 61 (1957) 93.
[55] R.-W. Lin, H.H. Johnson, in: Perspectives in Hydrogen in Metals, eds. M.F. Ashby and J.P. Hirth (Pergamon, Oxford, 1986) p. 225.
[56] M. Surkein, R. Heidersbach, in: Advanced Techniques for Characterizing Hydrogen in Metals, eds. N.F. Fiore and B.J. Berkowitz (Metallurgical Society of AIME, 1982) p. 119.
[57] A.J. Kumnick, H.H. Johnson, Metall.Trans. 5 (1974) 1199.
[58] H.H. Johnson, Metall. Trans. A19 (1988) 2371.
[59] H.H. Johnson, R.W. Lin, in: Hydrogen Effects in Metals, eds. I.M. Bernstein and A.W. Thompson (Metallurgical Society of AIME, 1981) p. 3.
[60] M.L. Hill, J. Met. 12 (1960) 69.
[61] J. Völkl, G. Alefeld, in: Hydrogen in Metals I, eds. G. Alefeld and J. Völkl (Springer, Berlin, 1978) p. 321.
[62] J.D. Hobson, J. Iron Steel Inst. 189 (1958) 315.
[63] G. Benamati, A. Donato, A. Solina, R. Valentini, S. Lanza, J. Nucl. Mater. 212–215 (1994) 1401.
[64] M.L. Hill, E.W. Johnson, Trans. Met. Soc. AIME 215 (1959) 717.
[65] B. Chew, Met. Sci. J. 5 (1971) 195.
[66] G.M. Pressouyre, I.M. Bernstein, Metall. Trans. A9 (1978) 1571.
[67] K.S. Forcey, I. Iordanova, D.K. Ross, Mater. Sci. Tech. 6 (1990) 357.
[68] G.M. Pressouyre, Metall. Trans 10A (1979) 1571.
[69] E. Serra, A. Perujo, K.S. Forcey, to be published.
[70] M.L. Hill, 47th Ann. Techn. Proc. Amer. Electroplaters Soc., 1960, p. 124, cited in Ref. [69].
[71] F.R. Coe, J. Moreton, J. Iron Steel Inst. 66 (1966) 366.
[72] D.H. Harries, G.H. Broomfield, J. Nucl. Mater. 9 (1963) 327.
[73] G. Benamati, in: Annual Report 1995, EURATOM-ENEA, ed. A. Donato, SDS4.2.1.
[74] R.B. McLellan, Scr. Metall. 15 (1981) 1251.
[75] E. Hashimoto, T. Kino, J. Nucl. Mater. 133&134 (1985) 289.
[76] J.F. Ziegler, Helium, Stopping Powers and Ranges in All Elemental Matter (Pergamon, Oxford, 1977) p. 45.
[77] H.H. Andersen, J.F. Ziegler, Hydrogen, Stopping Powers and Ranges in All Elemental Matter (Pergamon, Oxford, 1977) p. 21.